Heliyon 8 (2022) e09209

Contents lists available at ScienceDirect

Heliyon

journal homepage: www.cell.com/heliyon

Research article

Silver-doped active carbon spheres and their application for microbial decontamination of water

Harish Chandra Joshi [b], Dhiraj Dutta [a], Nisha Gaur [a], G.S. Singh [b], Rama Dubey [a,*], S.K. Dwivedi [a]

[a] Defence Research Laboratory, Post Bag No. 2, Tezpur, 784001, Assam, India
[b] Defence Materials and Stores Research and Development Establishment, Kanpur, 208 013, India

HIGHLIGHTS

- Novel low-density silver doped active carbon spheres (ACS) were synthesized successfully.
- Characterization and antibacterial activity was examined for water decontamination application.
- Results revealed that the material effectively reduced microbial load by 99.9 %.

GRAPHICAL ABSTRACT

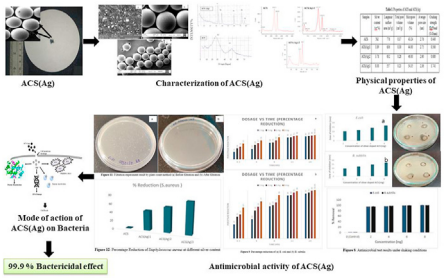

ARTICLE INFO

Keywords:
Silver nanoparticles
Resin
Carbonization
Activation
Antimicrobial assay

ABSTRACT

Highly efficient and durable, silver nanoparticles doped Active Carbon Spheres ACS(Ag) were synthesized by carbonization and activation of silver exchanged resins. The silver exchanged resins were prepared by exchanging H^+ ions of polystyrene sulphonate resin with Ag^+ ions of silver nitrate ($AgNO_3$). The quantity of Ag^+ in the spheres was controlled by varying the concentration of $AgNO_3$, from 0.0125 to 0.1 M. With increasing molar concentration of $AgNO_3$, the effective intake of Ag^+ by the sphere increases from 1.1 to 8.1 weight percent (wt %). For activation, the spheres were incubated in the CO_2 atmosphere for 6 h at fixed soaking temperature i.e. 1123 K. The characterization of synthesized silver doped ACS was performed by using different sophisticated instrumental techniques. The antimicrobial activity of silver doped ACS was studied against different bacterial strains like, *E. coli*, *B. subtilis* and *Staphylococcus aureus*. The study demonstrated that the zone of inhibition for *E. coli* was 16.9 ± 0.7 mm while for *B. subtilis* it was 17.1 ± 0.3 mm at a concentration of 8 mg of synthesized material. In addition, satisfactory results were obtained in shake flask and filtration test experiments also, even at a low concentration of 2 mg, showing growth inhibition of 94% for *E. coli and* 93% for *B. subtilis*. When the concentration of silver doped ACS was increased to 8 mg, complete removal of both the bacteria was observed after 24 h (100 % reduction for *E. coli* and *B. subtilis*). Furthermore, when silver doped ACS was tested against *Staphylococcus aureus* according to ASTM:E 2149-01 method, biocidal activity of up to 73% was observed. Therefore, the silver doped ACS can be considered as a potential biocidal material for the studied bacterial strains and hence find suitable application for decontamination of water.

* Corresponding author.
E-mail address: ramadubey.drl@gov.in (R. Dubey).

https://doi.org/10.1016/j.heliyon.2022.e09209
Received 30 March 2021; Received in revised form 9 August 2021; Accepted 25 March 2022

1. Introduction

Nowadays environmental pollution has become an area of concern due to its devastating effect on the life of planet. Different materials have been developed from time to time to combat this serious issue. Among them activated carbon has been widely used for the purification of both air and water (Bhave and Yeleswarapu, 2020; Hashim et al., 2019). It has been used in the form of powder, granules and spheres (Wan Ibrahim et al., 2019; Wickramaratne and Jaroniec, 2013). Activated carbon spheres (ACS) offer many advantages when compared to other forms of carbon like powder, granules etc, as they could provide perfect uniform filling geometry, higher mechanical strength, and low resistance to diffusion and flow of fluids in packed bed because of their homogenous piling in the bed (Singh and Lal, 2010). It has been reported that bacteria preferably adhered to the solid support made up of carbon materialor it may also grow on the activated carbon during the purification process (Kuroda et al., 1988; Wu et al., 2017). Silver is well-known for its antimicrobial properties hence several studies have been performed by using different types of silver coated materials to assess their antimicrobial efficiency (Altintig and Kirkil, 2016; Li et al., 2017).

Generally ACSs are synthesized by carbonization of a polymeric material without melting, under high-temperature conditions in the range of 800–1000 °C (Singh and Lal, 2010). In the present study, a commonly available polystyrene sulphonatecation exchange thermosetting resin was used as the precursor material. The precursor was modified by exchanging its H^+ ions with Ag^+ ions. Silver ions can be easily exchanged with such resin by simply treating it with an aqueous solution of silver salt such as silver nitrate. Since ion exchange takes place at the atomic level, the particle size in the final product may be expected to be very small. After carbonization and activation of the precursor, silver particles are uniformly distributed throughout the carbon beads and tightly bound to the surface. Various parameters are involved in the preparation of silver doped ACS. They are the type and molecular weight of the raw material as well as method of its preparation including time, temperature and heating rate employed for the carbonization and subsequent activation. A proper choice of suitable precursor material, activating agent, and the processing parameters for both carbonization and activation play a very important role. Although Ag is known for its antimicrobial activity since ancient times, but according to BIS standard, the presence of silver above desirable level of 0.1 ppm can act as a contaminant for drinking water. Hence during synthesis of silver doped antimicrobial agents it has to be ascertained that silver is tightly adhered to the surface of the base material so that its leaching could be prevented (Burduş;el et al., 2018; Hadrup and Lam, 2014).

In the present study, the preparation, carbonization and activation of silver nanoparticles doped ACS was successfully carried out by ion exchange of standard polystyrene sulphonate resin with Ag^+ ions. In addition, the characterization of synthesized silver doped ACS was done by using several sophisticated instrumental techniques. The antimicrobial property of silver doped ACS was also studied against *E. coli*, *B. subtilis* and *Staphylococcus aureus*.

2. Experimental

2.1. Preparation of silver ion-exchanged resin

The raw resin selected was spherical (0.6–1.2 mm) polystyrene – divinylbenzene co-polymer cation exchange resin with sulphonic acid groups as an ion exchangeable site. The resin was washed with deionized water to remove excess free H^+ ions from the surface of the resin. An aqueous solution of silver nitrate (AR grade) of different molar concentrations (0.0125–0.1 M) was added to it. The mouth of the beaker was covered, and the solution was magnetically stirred for 24 h, after which the resin was separated by filtration. The exchanged resin was washed with deionized water 3 to 4 times to remove excess free Ag^+ ions present at the surface of the resin beads. Resin beads were further filtered and air-dried at room temperature to obtain free-flowing resin beads (Mohebbi et al., 2019; Ye et al., 2019).

2.2. Carbonization

The silver ion-exchanged resin was filled from one end into a tubular quartz reactor of size 800 mm length and 20 mm internal diameter over a quartz wool bed. Initially, the reactor was purged with N_2 gas at 423 K for 1 h to remove moisture and maintain an inert atmosphere. The resin was then heated at a heating rate of 5 K/min up to 593 K. This temperature was maintained for 2 h for partial carbonization of the resin. The nitrogen flow rate was maintained in such a way as to fluidize the bed. Finally, the partially carbonized resins were heated at a rate of 3.5 K/min up to heat treatment temperature (HTT) of 1123 K(Y. H. Li et al., 2020).

During the process, volatilization of various organic compounds present in the resin takes place, giving rise to porous carbon beads. The adsorptive power of the char obtained after carbonization was low due to the deposition of tarry substances and disorganized carbon in the pores. Hence, to increase the adsorptive power of carbonized char, controlled oxidation was carried out by suitable oxidizing gases at elevated temperatures. This process is known as activation (Zhai et al., 2020).

2.3. Activation

The most commonly used oxidizing gases for activation are carbon-dioxide and steam. Initially, while activation of char, the disordered carbon is removed, after which the surface of elementary crystallites gets exposed to the activating agent. The closed pores are opened, and existing pores are enlarged during activation. In the present study, CO_2 was used as an activating agent because it creates only microporosity due to its slow reactivity during the whole activation period. A definite mass of the carbonized resin was filled in the reactor for activation by theCO_2 stream. The flow rate of carbon-dioxide gas was maintained at 500 cm^3/min together with sufficient nitrogen gas for fluidization of the bed. The flow rate of gases, which enter the reactor, was regulated using a set of the mass flow controller. The gas flow was continued for 6 h at 1123 K. The ACS thus obtained was allowed to cool to room temperature in a nitrogen atmosphere and then removed from the reactor. Raw ion exchange resin (H^+ type) was also carbonized and activated under the same set of operative conditions. The particle size of the ACS was in the range of 0.3–0.6 mm. The ACS and silver doped ACS were characterized by several instrumental techniques as reported in previous studies (Yue and Economy, 2017).

2.4. Measurements

The particle size of ACS and silver doped ACS i.e., ACS (Ag) samples was determined by using different mesh size sieves of ASTM standard. The silver content of ACS (Ag) samples was determined by using the standard gravimetric method.

At 77 K nitrogen adsorption/desorption isotherms were measured using the Micromeritics ASAP-2020 instrument to determine the morphological properties of ACS samples. Each sample was degassed at 573 K under vacuum (10^{-6} mm of Hg) for 4 h before starting each measurement. The surface morphology of the ACS(Ag) was observed by utilizing scanning electron microscopy. Powder X-ray diffraction (PXRD) of the ACS and ACS (Ag) samples were measured to determine the structural parameters using Ni filtered Kα radiation ($\lambda = 0.154$ nm) operating at 30 kV and 20 mA. Sherrer's equation was used to compute the crystal size from the broadening of the peak corresponding to (111) reflection. The crushing strength of samples was measured using a crushing strength tester as per ASTM (C-695 & E-4) standard (H. Y. Li et al., 2020; Mohamed et al., 2020; Réti et al., 2017).

2.5. Preparation of bacterial suspensions

Gram-Negative bacteria *Escherichia coli* (MTCC 443) and Gram-positive *Bacillussubtilis* (MTCC 1305) were selected as the model

organism to check the antimicrobial property of silver doped ACS. For each species, 50 ml of nutrient broth was prepared by inoculating the 100 µl of an overnight culture (OD-0.6 nm) for 12 h. The prepared overnight bacterial cultures were used for the antimicrobial assay.

2.5.1. Agar well diffusion assay

The antimicrobial test on the silver doped ACS was performed by using an agar well diffusion assay. After autoclaving, nutrient agar media was used to culture the bacteria. 100 µl of the freshly prepared bacterial culture (*Escherichia coli* and *Bacillussubtilis*) was spread on the nutrient agar plate. After solidification, a well of 6 mm diameter was punched using a sterile cork borer. 10 mg of different amounts of ACS and different amounts of silver doped ACS (2,4,6,8 mg) were loaded in the well. Later, the plates were incubated for 12 h at 37 °C, and the diameter of the zone of inhibition was documented in millimeters (mm). All the experiments were conducted thrice, with the result represented as the mean and standard deviation values (Charannya et al., 2018).

2.5.2. Dynamic contact method for antimicrobial test

5 ml of the stock culture (CFU~ 10 ^{8}cells/ml) was pellet down at 1000 rpm for 5 min and the supernatant layer was discarded. To remove the residual broth, the pellet was washed thrice with distilled water. To makeup the stock volume the pellet was resuspended with 5 ml of the distilled water. 10 µl of bacterial stock culture along with a different concentration of silver-coated ACS and 2 ml of distilled water were filled in 10 ml test tubes. The test tubes were incubated at 150 rpm for 24 h at 37 °C. After incubation, the samples were tested for microbial presence by the standard plate count method (Bartram, 2013; Martí et al., 2018).

2.5.3. Effect of silver doped ACS concentration on bacteria removal

The effect of silver doped ACS concentration on removal efficiency of bacteria was calculated by Eq. (1):

$$\textit{Percentage Reduction} = \frac{(A-B)}{A} \times 100 \quad (1)$$

While the log reduction was calculated by Eq. (2)

$$\text{Log Reduction} = \log_{10}(A/B) \quad (2)$$

where A = number of viable cells before treatment.

B = number of viable cells after treatment.

2.5.4. Filtration test under gravity using burette

The antibacterial efficiency of silver doped ACS in real life was checked by fabricating a small filter by using a burette in which the synthesized material was kept on pre-sterilized glass wool layer at the bottom. The 100 ml of the sample was passed through it and the presence of the microbes in the filtered and unfiltered sample was counted using colony-forming unit per ml (CFU/ml) (Bartram, 2013). The experimental setup of the filtration assembly used for the antimicrobial study is shown in Figure 1.

3. Results and discussion

3.1. Visual appearance of the sample

The visual observation of the silver doped ACS sample is displayed in Figure 2. Both the doped and the undoped ACSappear blackish in color. This is due to the fact that the silver was doped in the ACS and not coated on the surface therefore, the color change was not observed.

3.2. Scanning electron microscopy (SEM)

Results of SEM examination are shown in Figure 3. The micrographs were taken at different magnifications from 11000X to 100X. The size of the spheres was observed to be in the range of 450–500 µm.High magnification images display the presence of silver in the form of patches distributed throughout the whole surface. At highest magnification of 11000X the surface showed bright regions distributed uniformly which indicate the presence of the silver. Hence from SEM micrographs it becomes evident that silver has been deposited uniformly in the ACS.

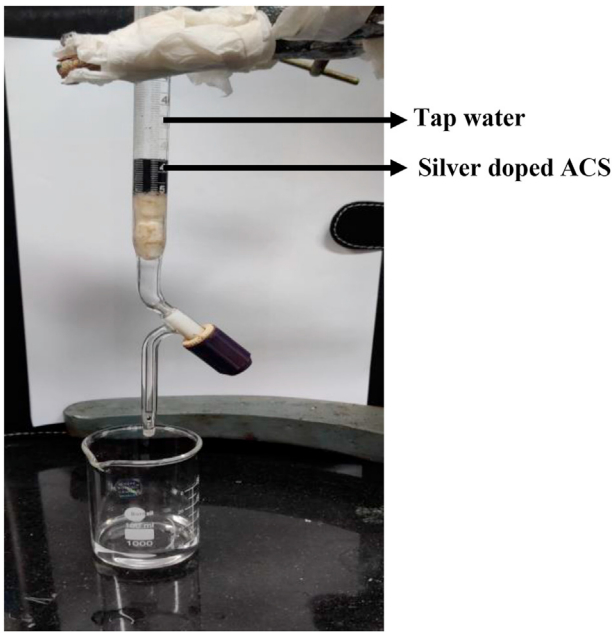

Figure 1. Experimental setup of filtration method.

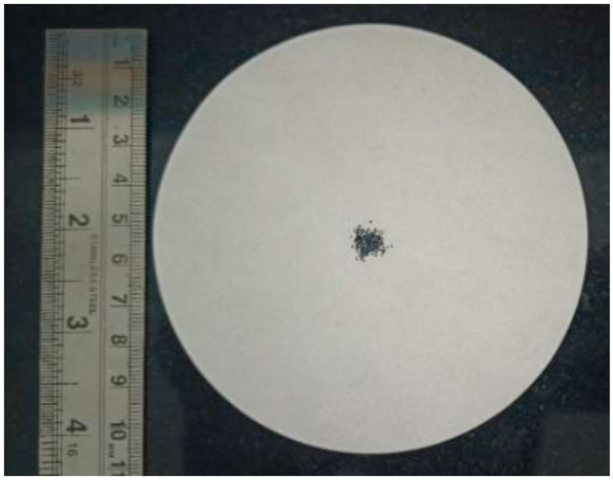

Figure 2. Digital image of silver doped ACS.

3.3. X-ray diffraction

The XRD pattern of the plain ACS and silver nanoparticles doped ACS sample is shown in Figure 4. Peaks of silver metal appeared in silver doped ACS. Scherrer's equation (Eq. (3)) using a half bandwidth of the diffraction peak around 38^{0} gave a silver crystallite size of 11.82 nm for the silver doped ACS sample.

$$t = K\,\lambda / (B\,\text{Cos}\theta) \quad (3)$$

where t is the average dimension of crystallite; K is the Scherrer constant, somewhat arbitrary value that falls in the range 0.87–1.0 (it is usually assumed to be 1); λ is the wavelength of X-ray, and B is the integral breadth of a reflection (in radian 2θ) located at 2θ.

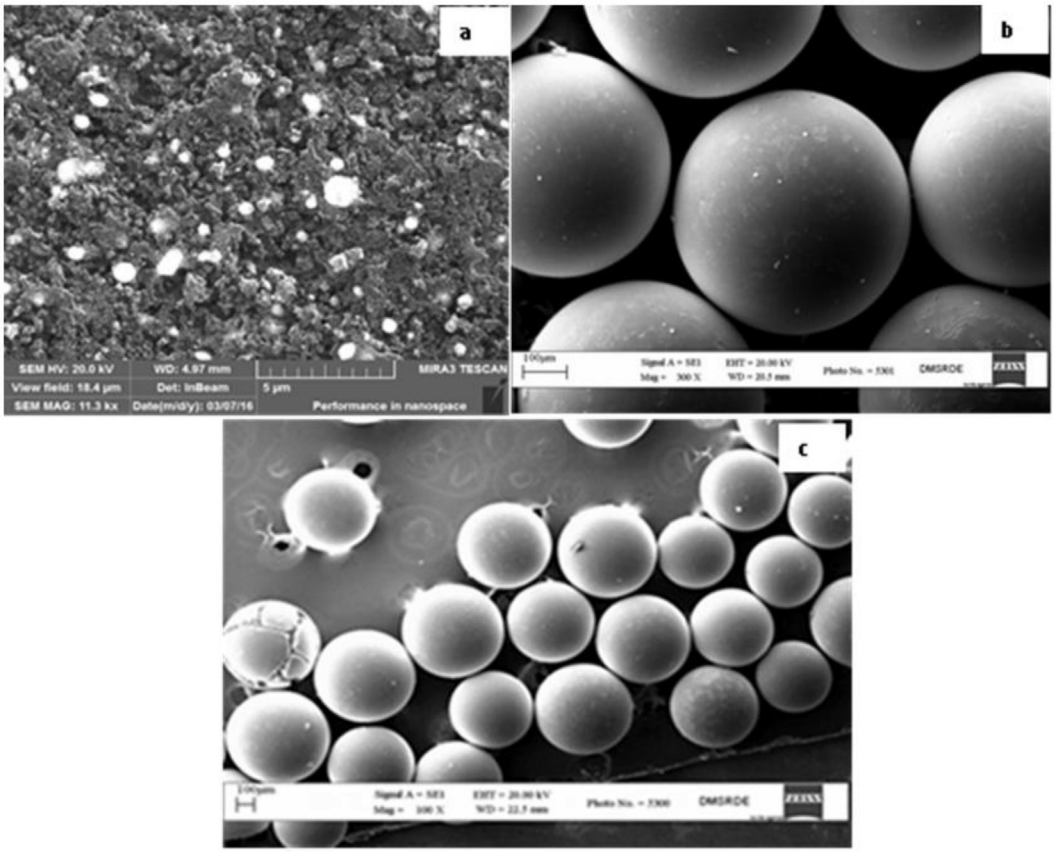

Figure 3. SEM micrographs of silver doped ACS at (a) 11.3 KX (b) 300 X (c) 100X.

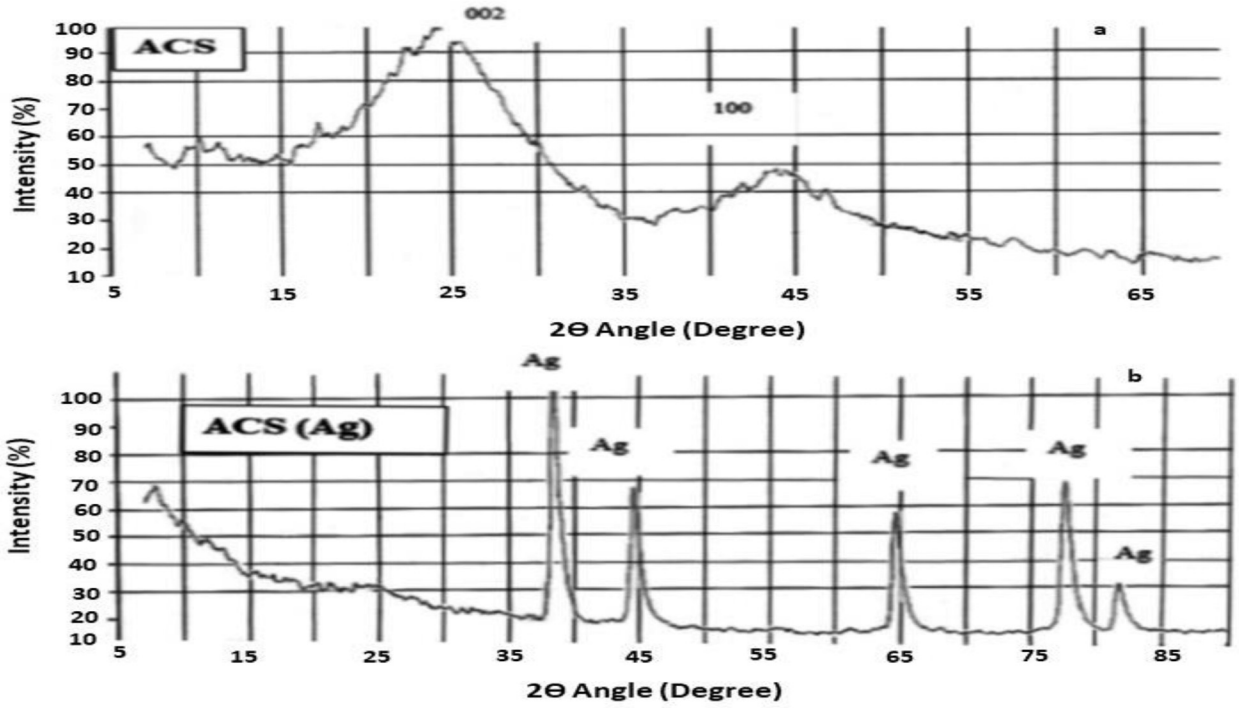

Figure 4. X-ray diffraction patterns of ACS (a) and ACS(Ag) (b).

From XRD studies of silver doped ACS sample, only metallic silver was found but no silver ion and silver oxide/sulfide were detected. The temperature at which carbonaceous resin is carbonized affects not only the yield, surface area, and pore structure of the resin, but also the dispersion of silver and the metal's interaction with the carbon support. During the carbonization, the exchanged silver ions are reduced to metallic silver.

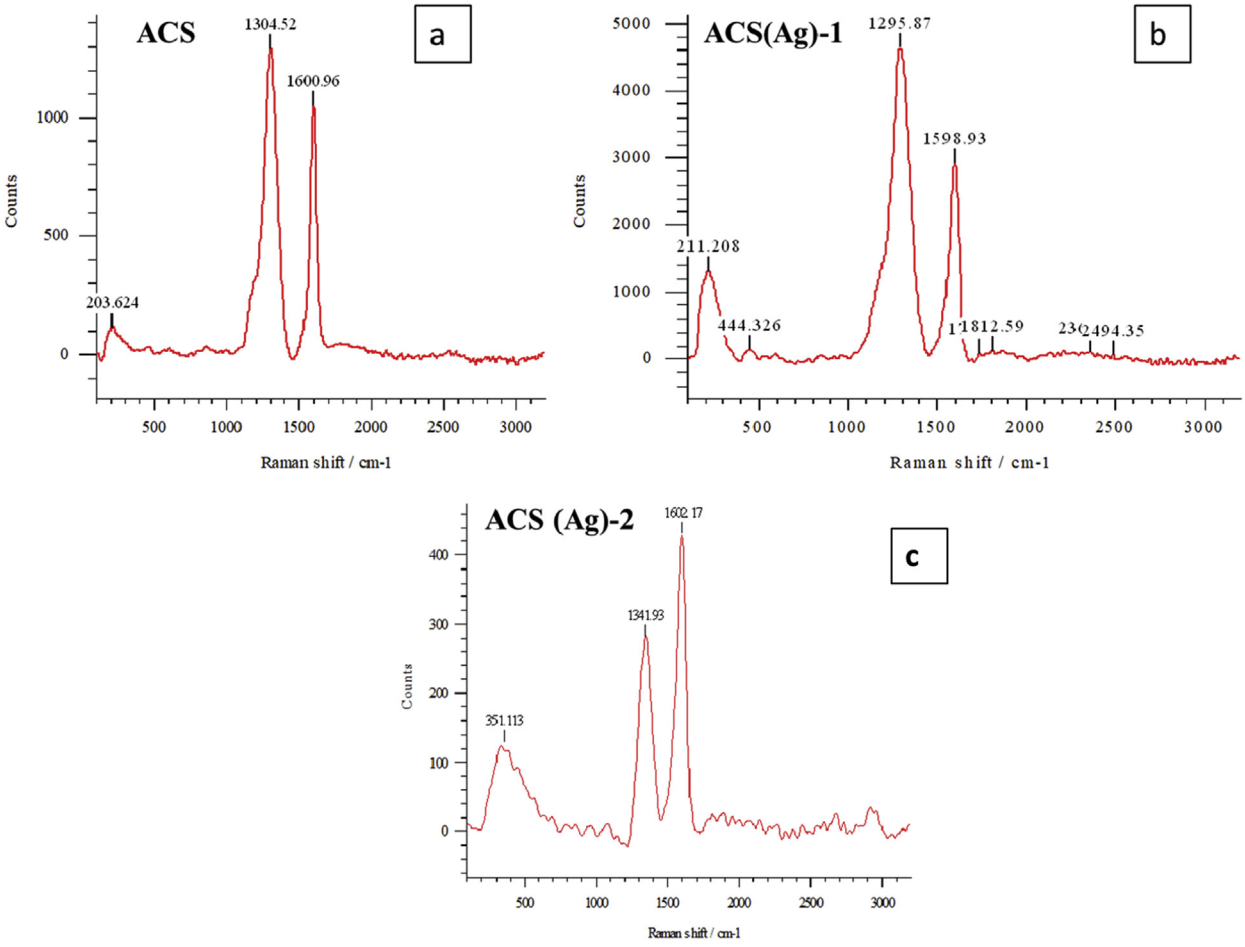

Figure 5. Raman spectra of ACS (a), ACS(Ag)-1 (b) and ACS (Ag)-2 (c).

The X-ray diffraction pattern of ACS obtained from H^+ resin show broad diffraction peaks corresponding to $2\theta = 22^0$ and $2\theta = 44^0$ which are assigned to disordered graphitic 002 plane and 100 planes respectively. This result indicates that silver ions existing as metal sulphonates in the starting resin prevent the development of graphite-like structure during carbonization in silver exchanged resins (Manikandan et al., 2006).

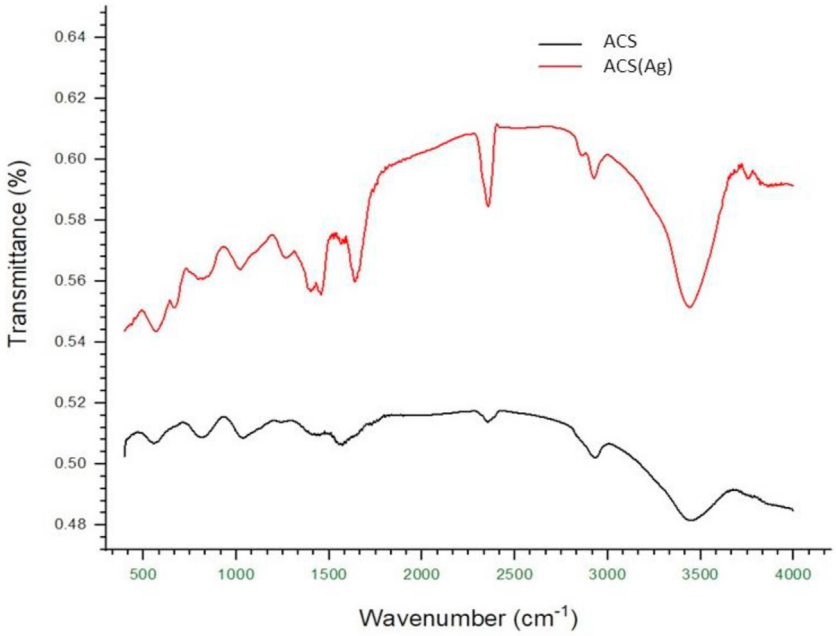

Figure 6. FTIR spectra of ACS and silver doped ACS.

Table 1. Properties of ACS and ACS(Ag).

Samples	Silver content (wt %)	Langmuir surface area (m^2/g)	Total pore volume (cm^3/g)	Micropore volume (%)	Average pore size (nm)	Crushing strength Kgf/bead (0.45 mm)
ACS	Nil	776	0.37	43.24	2.76	0.440
ACS(Ag)1	1.09	636	0.30	44.00	2.75	0.560
ACS(Ag)2	3.78	632	0.28	46.00	2.60	0.680
ACS(Ag)3	8.08	557	0.23	54.35	2.36	1.741

3.4. Raman spectroscopy

Raman Spectra of ACS and ACS(Ag) are presented in Figure 5. It was observed that the two main graphitic peaks were present in both ACS and ACS (Ag) samples along with other additional peaks for the latter. For ACS the D peak of disordered graphite structure was observed at 1304 cm-1, and the G peaks of sp2 bonded carbon atoms bonded in the hexagonal lattice at 1600 cm-1. The ID/IG ratio was around 1.23, indicating a large number of structural defects. ID/IG ratio of CNSs has been reported (Suzuki and Yoshimura, 2017) to be around 0.86 to 1.20. For silver doped ACS, a much higher ID/IG ratio of 1.58 indicated further changes in structure (Rubim et al., 1989) due to the presence of silver.

3.5. Fourier transform infrared spectroscopy (FTIR)

The FTIR spectra of ACS and silver dopedACS microspheres were recorded within the range of 500–4000 cm-1as shown in Figure 6. The band at3300-3500 cm-1 corresponds to stretching vibrations of isolated surface –OH moieties and/or –OH in alcohol and phenols. The band observed in the range of wavenumber 2830-3000 cm-1 can be assigned to C–H stretching (alkanes) while the bands in the range of 1500–1845 cm-1 are due to the presence of C=O groups (carboxylic acid, ketone/quinone) and C=C (aldehydes). In addition, the bands in the range of 950–1300 cm-1 corresponds to C–O stretching and O–H bending in various chemical surroundings while the bands in the range of 675–900 cm-1 can be assigned as C–H bending in aromatic compounds.

The various functional groups present in the ACS were hydroxyl, alcohol, phenol, alkanes, ketones, aldehyde, carboxylic acid esters, ethers and aromatic compounds. After doping of ACS with silver, the broadening of peaks was considerably reduced while significant increase in intensity was observed. This shows that the presence of silver affects the functional groups on the surface of ACS.

3.6. Effect of concentration of silver nitrate solution on the loading of silver

The silver content in silver doped ACS samples is shown in Table 1. From the table, it can be seen that silver content increases in the ACS by increasing the molar concentration of silver nitrate from 0.0125 to 0.1 M. Although, the exact mechanism is not well understood but it may probably be due to the limited solubility of the salt in water at ambient temperature. On increasing the salt concentration in the solution, the ionization of the salt would be suppressed as a result of which a sufficient quantity of silver ion would not be available in the solution for exchange with hydrogen ions.

3.7. Effect of silver content on the surface area

The specific surface area and silver content are the basic parameters, which are directly related to the capacity and capability of antimicrobial property of silver doped ACS samples. According to IUPAC recommendations, the Langmuir and the "t" method of Lippens were used for microporous materials, surface area and micropore volume calculation and the same parameters of ACS are summarized in Table 1(Lippens and de Boer, 1965).

From Table 1 it can be observed that surface area decreases from 776 to 557 m^2/g as the silver loading increases from 1.09 to8.08wt%. This may be due to exchange of silver ions with hydrogen ions throughout the structure of the resin beads, which during carbonization act as pillars between micro-crystallites which increase the microporosity by inhibiting the sintering effect at high temperature. But those silver ions which are filled inside the pores due to exposure of resin with a concentrated solution of silver nitrate attributed to a decrease in surface area by blocking the mouth of some micropores. The char yield (wt. %) remains constant at around 50 wt% based on dried raw resin for all the resins loaded with different wt.% of silver. The average pore size of ACS

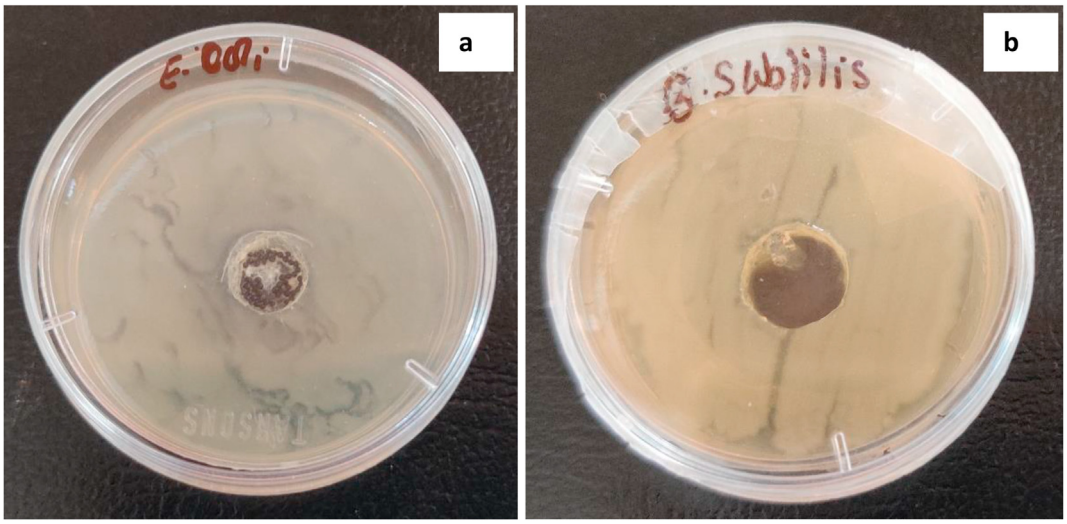

Figure 7. Zone of inhibition of (a) *E. coli* and (b) *B. subtilis* against undoped ACS.

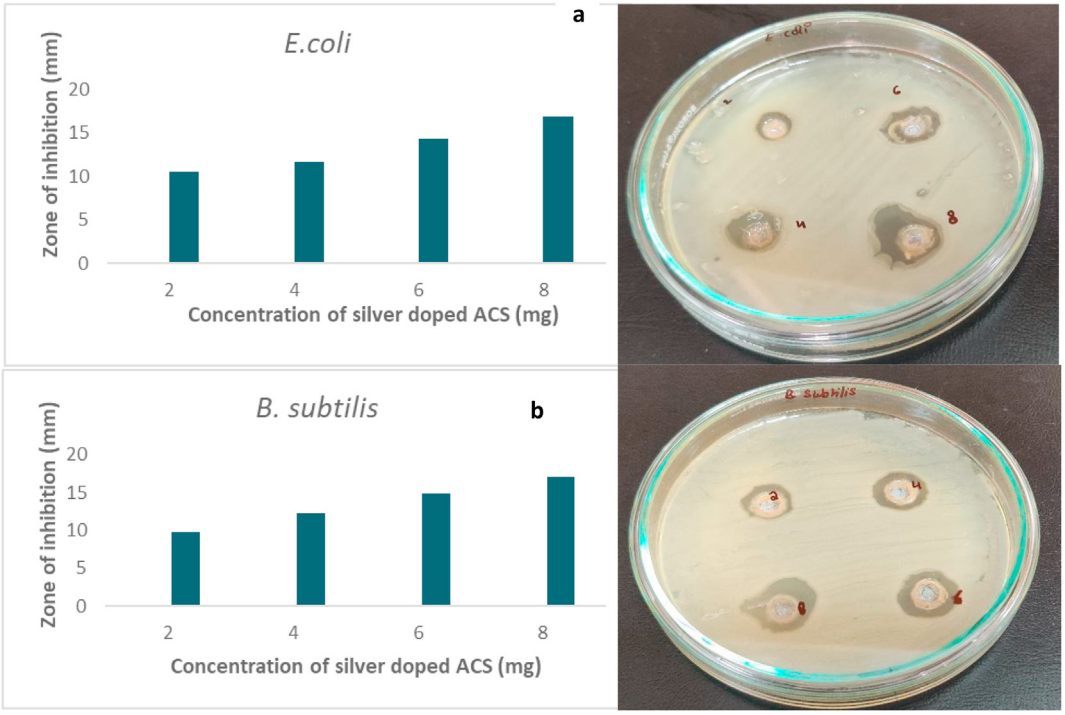

Figure 8. (a) & (b) shows the zone of inhibition against *E. coli* and *B. subtilis*.

decreases with the increase in the amount of silver content. So, this study reveals that the presence of silver also affects the pore size of ACS.

3.8. Effect of silver content on crushing strength

The shape and hardness are essential factors for practical utilization of the ACS. Low resistance to attrition will cause the removal of silver particles from the surface of the ACS. The effect of silver loading in ACS on their hardness is shown in Table 1. Here it can be seen that, as the silver content increases its crushing strength also increases as expected. It may be due to the pillar effect. However, higher content of silver is not desirable due to a decrease in surface properties of ACS. The ACS prepared from the silver exchanged resin maintains a spherical shape and becomes very hard. These results show that the ACS prepared from silver exchanged resins can be well utilized for practical purposes (Annaz et al., 2020).

3.9. Antimicrobial property of silver doped ACS

To check the efficiency of silver doped ACS as a decontaminating agent, different antibacterial tests were performed.

3.9.1. Plate assay and dynamic contact method

The undoped ACS showed no zone of inhibition against *E. coli* and *B. subtilis* as shown in Figure 7a,b respectively. However, in the case of silver doped ACS both the bacteria showed antimicrobial activity. This might be due to the presence of silver in ACS.

The results of the inhibitory effect of silver doped ACS against *E. coli* and *B. subtilis studied* by plate assay method are shown in Figure 8a,b respectively. The histograms are also shown displaying relation between sample concentration and zone of inhibition. The findings of this research revealed that silver doped ACS is a potential antimicrobial agent. The

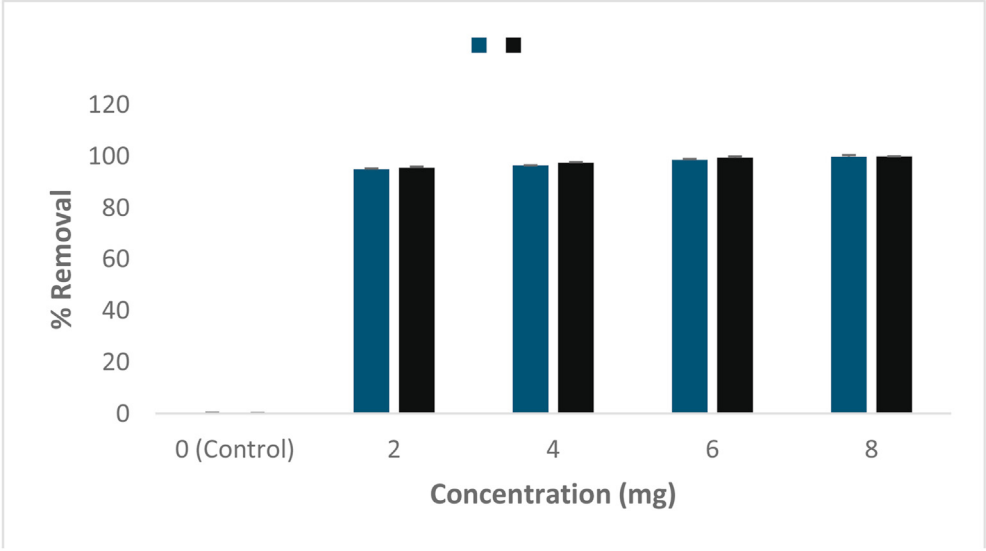

Figure 9. Antimicrobial test results under shaking conditions.

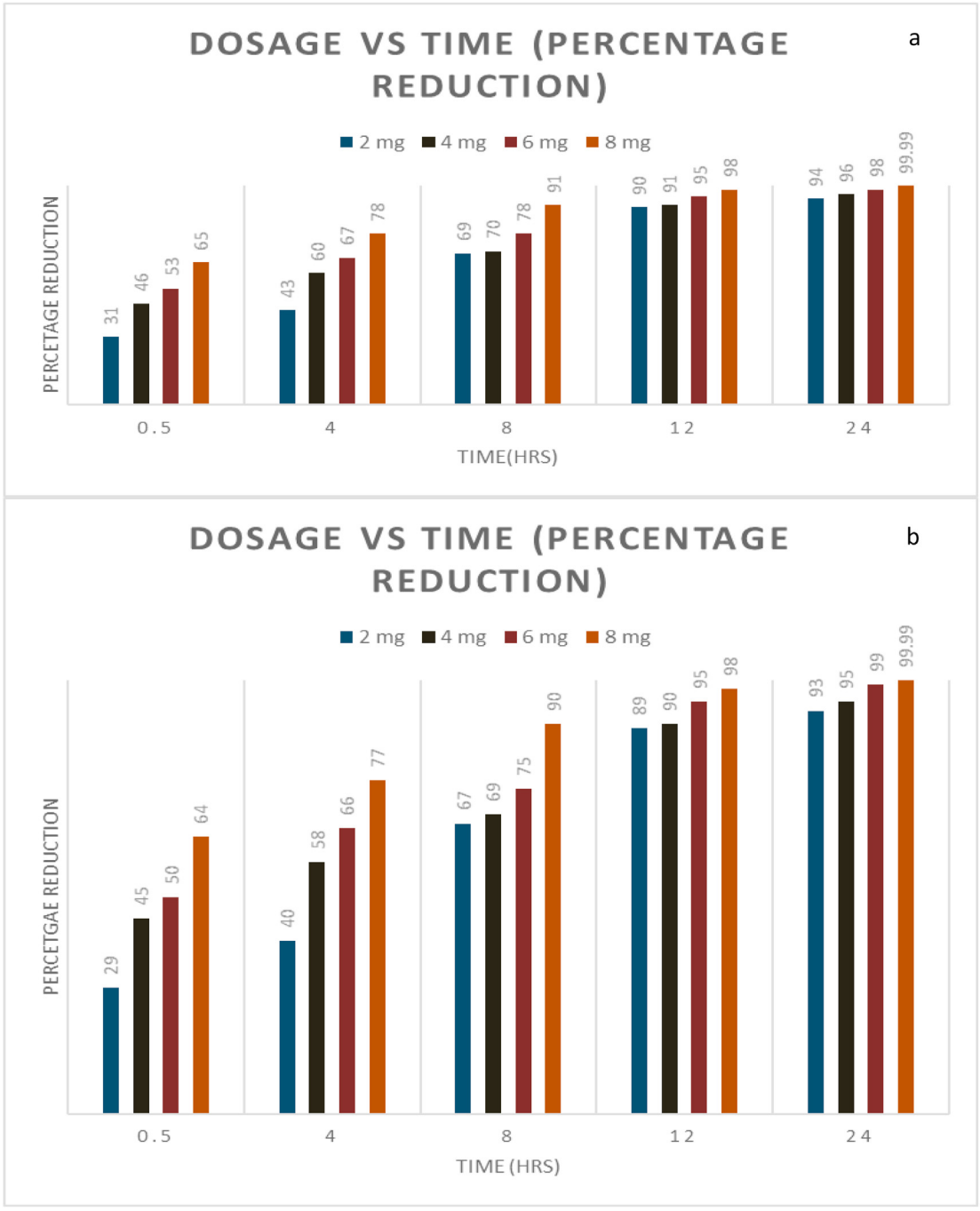

Figure 10. Percentage reduction of (a) *E. coli* and (b) *B. subtilis*.

diameter of the zone of inhibition against *E. coli* was 10.6 ± 0.3, 11.7 ± 0.4, 14.3 ± 0.5, and 16.9 ± 0.7 mm for the concentrations 2, 4, 6, and 8 mg of silver doped ACS respectively. While in case of *B. subtilisthe* zone of inhibition was 9.8 ± 0.4, 12.3 ± 0.2, 14.9 ± 0.6, and 17.1 ± 0.3 mm for the same above-mentioned concentrations.

The antibacterial effect for different concentrations of silver doped ACS against *E. coli* and *B. subtilis* under dynamic conditions (shaking time 24 h, *E. coli* and *B. subtilis* concentration (10^8 CFU/ml), and contaminated solution (100 ml) are shown in Figure 9. It was observed that the growth of bacterial cells was inhibited by silver doped ACS after contacting for 24 h which proves the bactericidal effect of silver doped ACS against both *E. coli* and *B. subtilis*. These results are in line with the previous studies (Ghiuț;ă et al., 2018).

To study the effect of silver doped ACS on bacterial strains, its concentration was varied from 2 to 8 mg as shown in Figure 10 and Figure 11. By plate agar method it was observed that the undoped ACS does not have any effect on the bacterial growth. But the silver doped ACS showed bactericidal activity (*E. coli*- 94 % and *B. subtilis*- 93%) even at low concentration (2 mg). When the concentration was increased to 4 mg, the percent reduction also increased to 96 and 95% for *E. coli* and *B. subtilis* respectively. Additionally, the percent reduction was further increased to 98 and 99% for *E. coli* and *B. subtilis* respectively on increasing the amount to 6 mg. When the silver doped ACS amount was further increased to 8 mg, 100 % reduction was observed after 24 h of incubation with 100 ml of contaminated solution (Pazos-Ortiz et al., 2017).

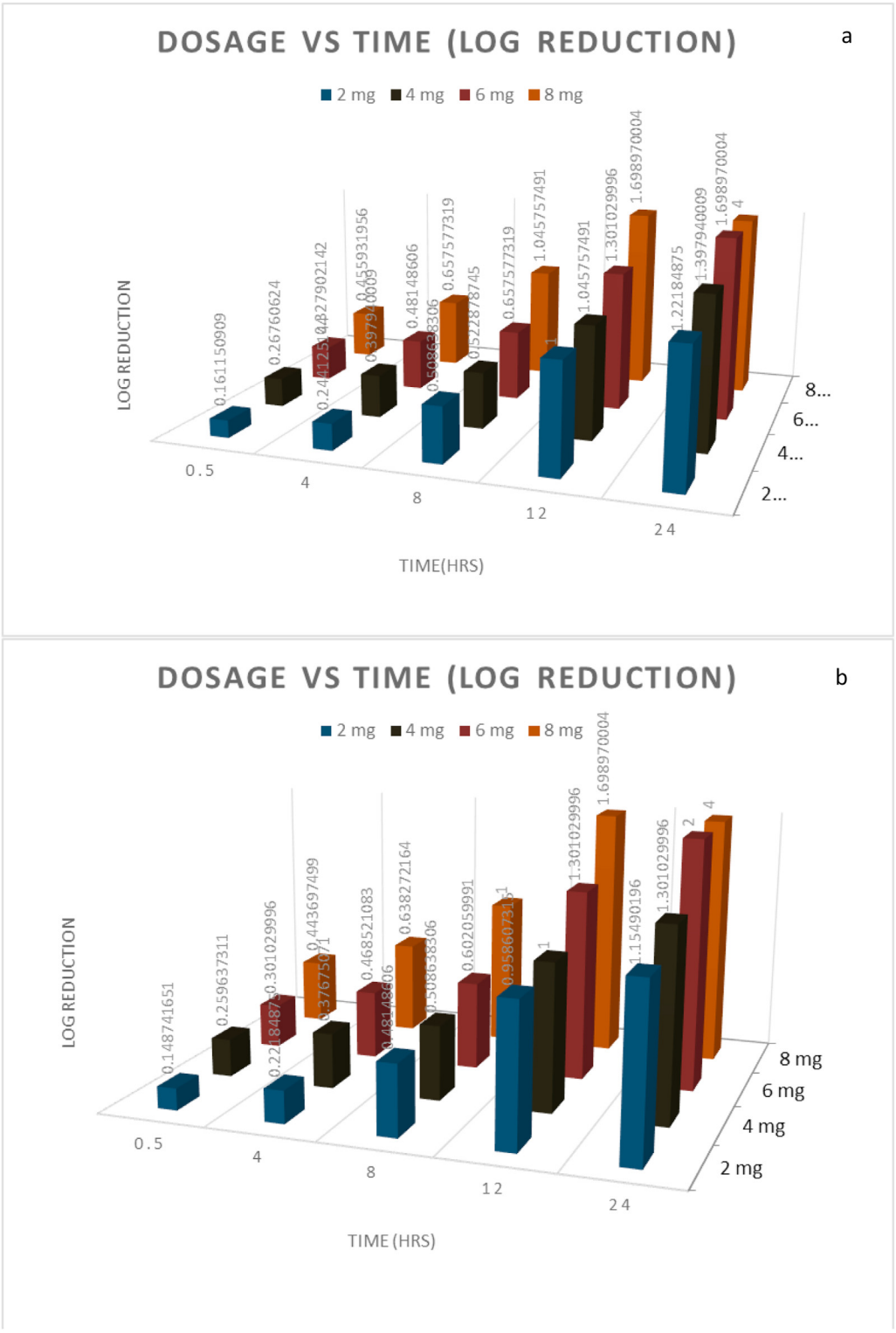

Figure 11. Log reduction of (a) *E. coli* and (b) *B. subtilis*.

3.9.2. Filtration test experiment

In this experiment tap water was used, and the antimicrobial activity of silver doped ACS was evaluated against *E. coli* and *B. subtilis*. The results showed that the synthesized material display eda 100% reduction of both the bacteria. Further, tap water was used to check the broad spectrum of present microbes and it was found that before filtration the bacterial count was $1.6 * 10^7$ CFU/ml while after filtration no growth was observed as mentioned in Figure 12.

3.9.3. Antimicrobial activity using S. aureus

Staphylococcus aureus is a bacteria that dwells on the skin and can cause everything from pimples to boils, folliculitis, furuncles, carbuncles,

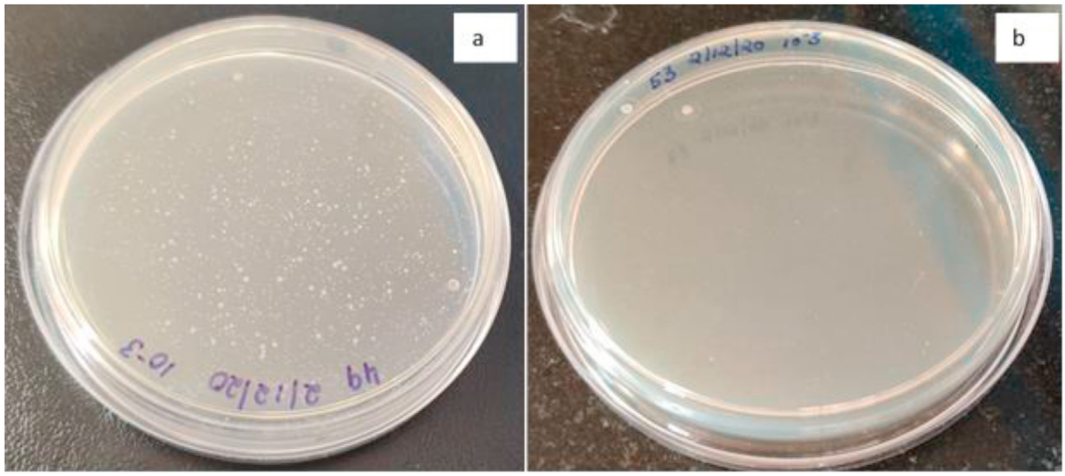

Figure 12. Filtration experiment result by plate count method (a) before &(b) after filtration.

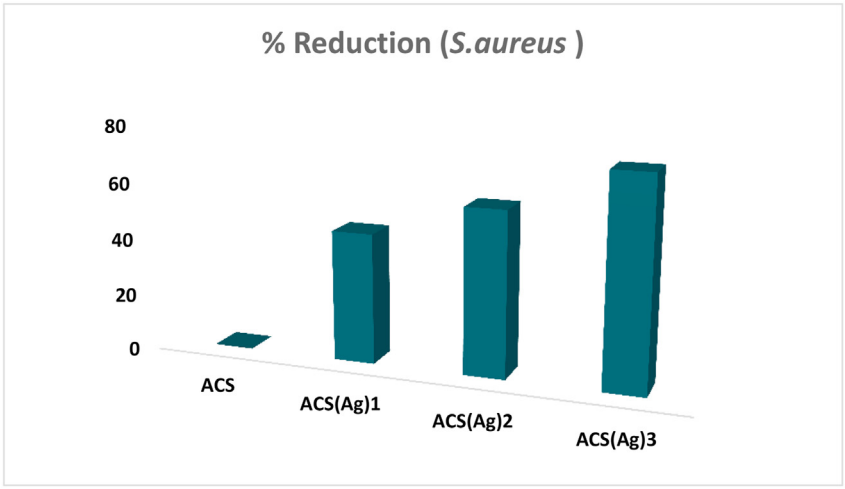

Figure 13. Percentage reduction of *Staphylococcus aureus* at different ACS(Ag) concentration.

scalded skin syndrome, and abscesses, as well, resulting in life-threatening conditions including pneumonia and septicemia. Therefore, in the present study *S. aureus* was also used to evaluate the antimicrobial activity of ACS and ACS(Ag) using the standard ASTM: E2149-01 test method. The results of antibacterial activity of silver doped ACS against *S. aureus are* shown in Figure 13 where it was observed that the antibacterial property of ACS increases with increase in silver content and more than 70% of the bacteria could be eliminated by incorporating 8 mg of ACS(Ag).

In addition to application of this material for water decontamination it can also be used for functional textiles. Thus, protective clothing made out of this silver nanoparticle doped ACS could act as bio-protective wear for kids, patients, and even for doctors. It is reasonable to consider that ACS(Ag) can act as a promising material for air and water purification. This work could give further opportunities in terms of clothing against biological warfare agents and medical textiles.

3.9.4. Mode of action of silver doped ACS on a bacterial cell wall

Components of the membrane and cell wall exert different adhesion pathways for silver doped activated carbon spheres. The main function of the cell wall and membrane is to protect the microbes against environmental threats. The difference in the bacteria is due to the composition of its cell wall and depending on this they are classified as Gram-negative and Gram-positive. The Gram-negative cell wall contains at least two lipopolysaccharides layers while Gram-positive contains athick peptidoglycan layer. Generally, silver doped ACS shows higher antibacterial activity against Gram-negative as compared to Gram-positive bacteria. This might be due to the presence of a thick peptidoglycan layer in the Gram-positive bacteria which is made of glycan strands cross-linked by short peptides and anionic glycopolymers called teichoic acid. This peptidoglycan layer provides a natural barrier for the penetration of silver doped ACS in bacteria. In contrast to Gram-positive bacteria, Gram-negative bacteria have a thinner cell wall and fewer peptidoglycan content (Estevez et al., 2019; Fernando et al., 2018).

The mechanism of action of silver doped ACS on the bacterial cell wall is presented in Figure 14. The interaction between the silver doped ACS and bacteria starts with the adhesion of Ag to the microbial cell wall. The adhesion between the Ag (positive or less negative charged) and cell wall of bacteria (negatively charged) is based on electrostatic interaction. This interaction leads to the morphological changes in the cell membrane which triggers the disruption of membrane permeability and respiratory function, finally leading to death of the cell. Additionally, with increase in disruption of cellular permeability and cell wall disruption, the cellular components such as DNA, protein, enzymes, and ions leak into the environment (Dadi et al., 2019; Fernando et al., 2018). Thus, all these process together result in destruction or death of the targeted microorganism.

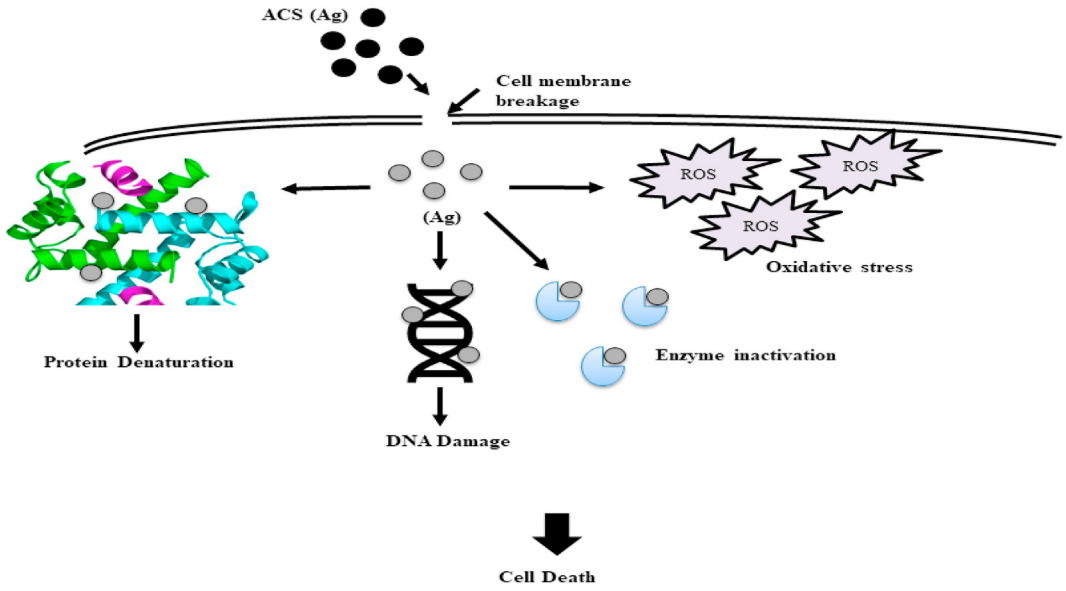

Figure 14. Mechanism of action of silver doped ACS on a bacterial cell wall.

4. Conclusions

The present study demonstrated that, silver nanoparticles doped ACS could be successfully prepared by carbonization, activation and silver doping of polystyrene sulphonate resin. The presence of silver in precursor controls the rate of activation, which results in higher yield and better mechanical strength as compared to plain (H^+ type) resin. The presence of silver also prevents the development of graphite-like structures during processing. The average crystallite size of the silver in ACS(Ag) was 11.82 nm, which suggests that the ion-exchange technique is useful to disperse fine silver particles in the active carbon spheres. The surface area of ACS was found to be 776 m^2/g which upon silver doping reduced to 557 m^2/g at a concentration of 8.08 wt%.The batch studies and zone of inhibition tests have established higher antimicrobial activity of the material (silver doped ACS) against the*E.coli* and *B. subtilis*. In addition, both the bacteria exhibited dose-dependent antimicrobial activity, and 8 mg was found to be an effective dose for complete removal of microbes from the water after 24 h. Hence, the Activated Carbon Sphere (ACS) is truly an efficient substrate for doping of silver to obtain economically viable material for water purification system. Further exploration of its application in the areas of air purification, wastewater management, and energy storage can also be undertaken.

5. Ethical approval and consent to participate

All work has been carried out with appropriate ethical approval and consent of participation has also been taken.

6. Consent for publication

Consent of publication has been taken from all authors.

Declarations

Author contribution statement

Harish Chandra Joshi, Dhiraj Dutta, Nisha Gaur, GS Singh: Conceived and designed the experiments; Performed the experiments.

Rama Dubey: Analyzed and interpreted the data; Wrote the paper.

SK Dwivedi: Contributed reagents, materials, analysis tools or data; Wrote the paper.

Funding statement

This research did not receive any specific grant from funding agencies in the public, commercial, or not-for-profit sectors.

Data availability statement

Data included in article/supplementary material/referenced in article.

Declaration of interests statement

The authors declare no conflict of interest.

Additional information

No additional information is available for this paper.

Acknowledgements

The authors sincerely acknowledge the kind help provided by the Director & testing team of DMSRDE, Kanpur for guidance in research work.

References

Altintig, E., Kirkil, S., 2016. Preparation and properties of Ag-coated activated carbon nanocomposites produced from wild chestnut shell by ZnCl2 activation. J. Taiwan Inst. Chem. Eng. 63, 180–188.

Annaz, A.A., Irhayyim, S.S., Hamada, M.L., Hammood, H.S., 2020. Comparative study of mechanical performance between Al–Graphite and Cu–Graphite self-lubricating composites reinforced by nano-Ag particles. AIMS Mater. Sci. 7 (5), 534–551.

Bartram, J., 2013. Heterotrophic plate counts and drinking-water safety: the significance of HPCs for water quality and human health. Water Int. 12. Online.

Bhave, P.P., Yeleswarapu, D., 2020. Removal of Indoor Air Pollutants Using Activated Carbon—A Review. Springer, Singapore, pp. 65–75.

Burdușel, A.-C., Gherasim, O., Grumezescu, A.M., Mogoantă, L., Ficai, A., Andronescu, E., 2018. Biomedical applications of silver nanoparticles: an up-to-date overview. Nanomaterials 8, 681.

Charannya, S., Duraivel, D., Padminee, K., Poorni, S., Nishanthine, C., Srinivasan, M.R., 2018. Comparative evaluation of antimicrobial efficacy of silver nanoparticles and 2% chlorhexidine gluconate when used alone and in combination assessed using agar diffusion method: an in vitro study. Contemp. Clin. Dent. 9.

Dadi, R., Azouani, R., Traore, M., Mielcarek, C., Kanaev, A., 2019. Antibacterial activity of ZnO and CuO nanoparticles against gram positive and gram negative strains. Mater. Sci. Eng. C 104, 109968.

Estevez, M.B., Mitchell, S.G., Faccio, R., Alborés, S., 2019. Biogenic silver nanoparticles: understanding the antimicrobial mechanism using Confocal Raman Microscopy. Mater. Res. Express 6.
Fernando, S., Gunasekara, T., Holton, J., 2018. Antimicrobial Nanoparticles: applications and mechanisms of action. Sri Lankan J. Infect. Dis. 8.
Ghiuță, I., Cristea, D., Croitoru, C., Kost, J., Wenkert, R., Vyrides, I., Anayiotos, A., Munteanu, D., 2018. Characterization and antimicrobial activity of silver nanoparticles, biosynthesized using Bacillus species. Appl. Surf. Sci. 438, 66–73.
Hadrup, N., Lam, H.R., 2014. Oral toxicity of silver ions, silver nanoparticles and colloidal silver – a review. Regul. Toxicol. Pharmacol. 68, 1–7.
Hashim, N.H., Teh, E.J., Rosli, M.A., 2019. A dynamic botanical air purifier (DBAP) with activated carbon root-bed for reducing indoor carbon dioxide levels. In: IOP Conference Series: Earth and Environmental Science. Institute of Physics Publishing, p. 12022.
Kuroda, M., Yuzawa, M., Sakakibara, Y., Okamura, M., 1988. Methanogenic bacteria adhered to solid supports. Water Res. 22, 653–656.
Li, H., Miao, Q., Chen, Y., Yin, M., Qi, H., Yang, M., Deng, Q., Wang, S., 2020. Modified carbon spheres as universal materials for adsorption of cationic harmful substances (paraquat and dyes) in water. Microporous Mesoporous Mater. 297, 110040.
Li, W.R., Sun, T.L., Zhou, S.L., Ma, Y.K., Shi, Q.S., Xie, X.B., Huang, X.M., 2017. A comparative analysis of antibacterial activity, dynamics, and effects of silver ions and silver nanoparticles against four bacterial strains. Int. Biodeterior. Biodegrad. 123, 304–310.
Li, Y., Wang, F., Miao, Y., Mai, Y., Li, H., Chen, X., Chen, J., 2020. A lignin-biochar with high oxygen-containing groups for adsorbing lead ion prepared by simultaneous oxidization and carbonization. Bioresour. Technol. 307, 123165.
Lippens, B.C., de Boer, J.H., 1965. Studies on pore systems in catalysts. V. The t method. J. Catal. 4, 319–323.
Manikandan, S., Majumdar, G., Chowdhury, D., Paul, A., Chattopadhyay, A., 2006. Solid-state storage of Ag nanoparticles in anion exchange resin beads and their recovery. J. Colloid Interface Sci. 295, 148–154.
Martí, M., Frígols, B., Serrano-Aroca, A., 2018. Antimicrobial characterization of advanced materials for bioengineering applications. J. Vis. Exp. 2018.
Mohamed, S.K., Abuelhamd, M., Allam, N.K., Shahat, A., Ramadan, M., Hassan, H.M.A., 2020. Eco-friendly facile synthesis of glucose–derived microporous carbon spheres electrodes with enhanced performance for water capacitive deionization. Desalination 477, 114278.
Mohebbi, A., Abolghasemi Mahani, A., Izadi, A., 2019. Ion exchange resin technology in recovery of precious and noble metals. In: Applications of Ion Exchange Materials in Chemical and Food Industries.
Pazos-Ortiz, E., Roque-Ruiz, J.H., Hinojos-Márquez, E.A., López-Esparza, J., Donohué-Cornejo, A., Cuevas-González, J.C., Espinosa-Cristóbal, L.F., Reyes-López, S.Y., 2017. Dose-dependent antimicrobial activity of silver nanoparticles on polycaprolactone fibers against gram-positive and gram-negative bacteria. J. Nanomater. 2017.
Réti, B., Kiss, G.I., Gyulavári, T., Baan, K., Magyari, K., Hernadi, K., 2017. Carbon sphere templates for TiO2 hollow structures: preparation, characterization and photocatalytic activity. Catal. Today 284, 160–168.
Rubim, J.C., Kannen, G., Schumacher, D., Dünnwald, J., Otto, A., 1989. Raman spectra of silver coated graphite and glassy carbon electrodes. Appl. Surf. Sci. 37, 233–243.
Singh, A., Lal, D., 2010. Preparation and characterization of activated carbon spheres from polystyrene sulphonate beads by steam and carbon dioxide activation. J. Appl. Polym. Sci. 115, 2409–2415.
Suzuki, S., Yoshimura, M., 2017. Chemical stability of graphene coated silver substrates for surface-enhanced Raman scattering. Sci. Rep. 7, 1–7.
Wan Ibrahim, W.M.H., Mohamad Amini, M.H., Sulaiman, N.S., Kadir, W.R.A., 2019. Powdered activated carbon prepared from *Leucaena leucocephala* biomass for cadmium removal in water purification process. Arab J. Basic Appl. Sci. 26, 30–40.
Wickramaratne, N.P., Jaroniec, M., 2013. Activated carbon spheres for CO2 adsorption. ACS Appl. Mater. Interfaces 5, 1849–1855.
Wu, C.C., Ghosh, S., Martin, K.J., Pinto, A.J., Denef, V.J., Olson, T.M., Love, N.G., 2017. The microbial colonization of activated carbon block point-of-use (PoU) filters with and without chlorinated phenol disinfection by-products. Environ. Sci. Water Res. Technol. 3, 830–843.
Ye, Z., Chen, L., Liu, C., Ning, S., Wang, X., Wei, Y., 2019. The rapid removal of iodide from aqueous solutions using a silica-based ion-exchange resin. React. Funct. Polym. 135, 52–57.
Yue, Z., Economy, J., 2017. Carbonization and activation for production of activated carbon fibers. In: Activated Carbon Fiber and Textiles. Elsevier Inc., pp. 61–139
Zhai, S., Jin, K., Zhou, M., Fan, Z., Zhao, H., Li, X., Zhao, Y., Ge, F., Cai, Z., 2020. A novel high performance flexible supercapacitor based on porous carbonized cotton/ZnO nanoparticle/CuS micro-sphere. Colloids Surface A Physicochem. Eng. Asp. 584, 124025.